Model Predictive Control of an Autonomous Underwater Vehicle in an *in situ* Estimated Water Current Profile

Lashika Medagoda, Stefan B. Williams
Australian Centre for Field Robotics
University of Sydney, Sydney NSW 2006 Australia
{l.medagoda,stefanw}@acfr.usyd.edu.au

I. Introduction

***Abstract*—Autonomous underwater vehicle control actuation is attained through the use of various methods, including propellors, jets and control surfaces. In order for a vehicle to achieve a desired trajectory and fulfil the mission goals successfully, the input of commands to the control subsystem is needed. Model predictive control (MPC) [2] relies on having a function which determines the future vehicle poses to a horizon given the present vehicle pose, and control actions during this time, and then minimising a cost function, such as the squared distance from the predicted to desired vehicle path. The advantage of MPC over other control methods like PID, Linear Quadratic Regulator (LQR) and its derivatives, is that very little hand tuning is required [10].**

The method outlined in [9] allows simultaenous estimates of the vehicle pose and the water current profile in the direction of the Acoustic Doppler Current Profiler (ADCP) beams, including small scale gradients *in situ*. The position, velocity, attitude and water current estimates from this localisation filter could be used to arrive at control commands in real-time to achieve the desired vehicle trajectory given the predicted water current acting on the vehicle and the vehicle pose for future states.

Results in this paper show that even with large delays due to the MPC optimisation stage to arrive at control actions, the controller can accurately track the desired trajectory in the mean estimates from the localisation. The trajectory following accuracy is shown to be limited by the localisation error.

Autonomous underwater vehicle control actuation is attained through the use of various methods, including propellors, jets and control surfaces. In order for a vehicle to achieve a desired trajectory and fulfil the mission goals successfully, the input of commands to the control subsystem is needed. Various control strategies exist, such as PID control which looks at the present vehicle pose and determines the control action given a reference state and hand-tuned gain parameters.

Model predictive control (MPC) [2] relies on having a function which determines the future vehicle poses to a horizon (for example 2 seconds into the future) given the present vehicle pose, and control actions during this time, and then minimising a cost function, such as the squared distance from the predicted to desired vehicle path. The advantage of MPC over other control methods like PID, Linear Quadratic Regulator (LQR) and its derivatives, is that very little hand tuning is required [10].

The method outlined in [9] allows simultaenous estimates of the vehicle pose and the water current profile in the direction of the Acoustic Doppler Current Profiler (ADCP) beams, including small scale gradients *in situ*. Figure 1 illustrates the estimation process. Thus these estimates could be used to arrive at control commands in real-time to achieve the desired vehicle trajectory given the predicted water current acting on the vehicle and the vehicle pose for future states. Additionally, Long Base Line (LBL) or Ultra Short Base Line (USBL) acoustic transponder positioning could be utilised to further reduce the error in the localisation.

This paper explores the application of MPC to follow a defined trajectory in the water column given the estimates of the position, velocity and attitude of the AUV, along with the water currents the vehicle will traverse through. The motivation for this application includes the ability to revisit a previously visited area of the ocean floor, or planning and executing a desired trajectory to sample and observe the mid-water column.

The remainder of this paper is organised as follows. Section II introduces the MPC theory and Section III the vehicle model applied. Section IV presents results to characterise the performance of the proposed method. Section V concludes with discussion of future direction and the implications of this work.

II. Model Predictive Control

The MPC method requires a vehicle model for the AUV, which allows the prediction of future vehicle poses given the present vehicle pose, water current map and control actions, to a certain control horizon. The smaller the control horizon, the faster the computation, but at the cost of being less optimal.

A cost function is then constructed which is to be minimised. The typical form for the cost function involves the difference between the predicted trajectory and the reference trajectory over the control horizon [11]:

$$J = \sum_{i}^{N} (r_i - x_i)^2 \tag{1}$$

where J is cost function to be minimised, x_i is the ith pose state, r_i is the reference state for x_i and N is the number of states in the cost function.

The derivatives of the pose states with respect to the control actions is then determined to aid in the optimisation procedure, which can be determined by determining the Jacobian of how the pose states evolve given the control actions.

An optimisation step is then conducted which finds the control actions which will minimize the sum of squares cost function in the control horizon.

978-1-4577-2091-8/12/$26.00 ©2011 IEEE

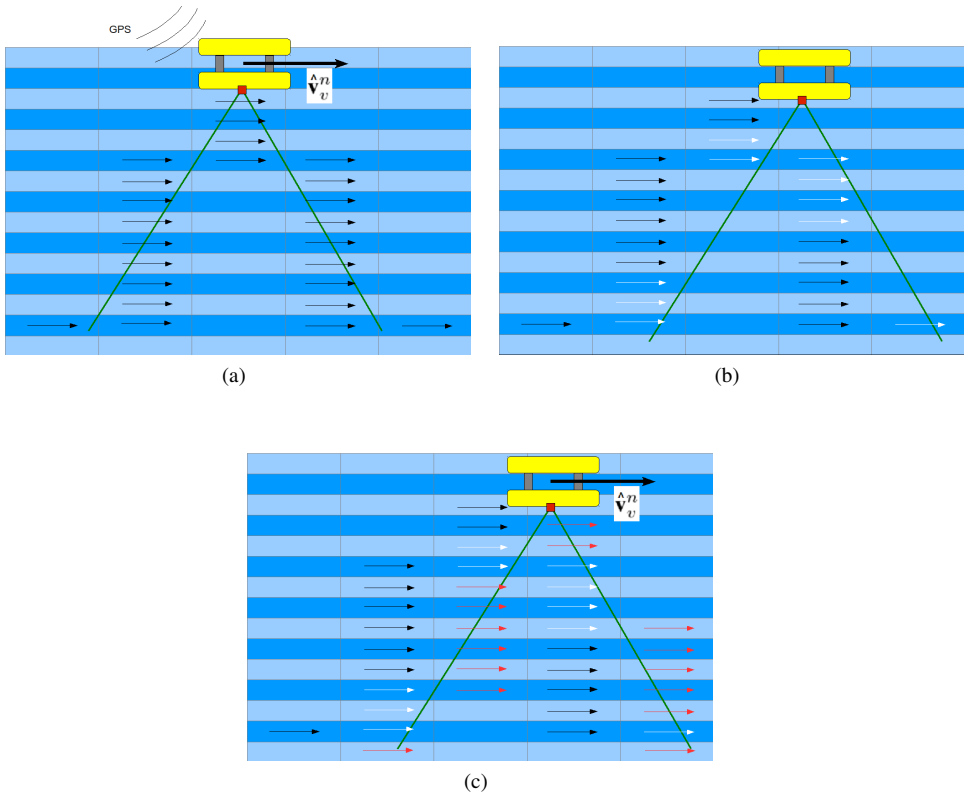

Fig. 1. ADCP aiding method sequence. The green lines are the ADCP beams, with the arrows representing estimates of the water current grids. (a) Initial GPS position and velocity are known, and water velocities with black arrows can be deduced. (b) The AUV moves underwater, losing GPS reception. Reobservation of some current grids occurs, shown as white arrows.(c) The AUV velocity in the world frame can be deduced, along with new current grids shown in red.

III. AUV VEHICLE MODELLING

To model the vehicle motion through the water current environment, it is assumed that the vehicle has differential thrust to control heading and forward velocity. The differential equation defining a 3DOF AUV model [3] with differential thrust such as the *Sirius* AUV [14] is:

$$\mathbf{M}\dot{\mathbf{v}} + \mathbf{C}(\mathbf{v})\mathbf{v} + \mathbf{D}(\mathbf{v})\mathbf{v} + \mathbf{C}_n^b(m\mathbf{g}^n + \mathbf{b}^n) = \boldsymbol{\tau} \quad (2)$$

$$\mathbf{v} = \begin{bmatrix} \dot{x_b} \\ \dot{y_b} \\ \dot{z_b} \\ \dot{\psi} \end{bmatrix} \quad (3)$$

$$\boldsymbol{\tau} = \begin{bmatrix} F_1 + F_2 \\ 0 \\ F_3 \\ F_1 r - F_2 r \end{bmatrix} \quad (4)$$

$$\mathbf{M} = diag\{M_x, M_y, M_z, I_z\} \quad (5)$$

$$\mathbf{C}(\mathbf{v}) = \begin{bmatrix} 0 & 0 & 0 & -M_y\dot{y_b} \\ 0 & 0 & 0 & M_x\dot{x_b} \\ 0 & 0 & 0 & 0 \\ M_y\dot{y_b} & -M_x\dot{x_b} & 0 & 0 \end{bmatrix} \quad (6)$$

$$\mathbf{D}(\mathbf{v}) = -diag\{D_{\dot{x}}|\dot{x_b}|, D_{\dot{y}}|\dot{y_b}|, D_{\dot{z}}|\dot{z_b}|, D_{\dot{\psi}}|\dot{\psi}|\} \quad (7)$$

where

- $\dot{x_b}$, $\dot{y_b}$ and $\dot{z_b}$ are the water relative velocities of the vehicle in the body frame in the forward, starboard and down directions respectively.
- $\dot{\psi}$ is the yaw rotational velocity of the vehicle
- $\mathbf{M}$ is the inertia matrix (including added mass)
- $\mathbf{C}(\mathbf{v})$ is the matrix of Coriolis and centripetal terms (including added mass)
- $\mathbf{D}(\mathbf{v})$ is the damping matrix
- $\boldsymbol{\tau}$ is the vector of control inputs
- F_1, F_2 and F_3 are the thrusts from the port, starboard and vertical thruster respectively
- m is the true mass of the vehicle
- $\mathbf{g}^n$ is the gravity vector in the navigation frame
- $\mathbf{b}^n$ is the buoyancy force in the navigation frame

In lieu of previously accurately derived vehicle parameters, they are estimated using [7] as a baseline. The parameters of the vehicle model used in the simulation are:

Symbol	True value
M_x	500 kg
M_y	500 kg
M_z	225 kg
I_z	179.049 kg m^2
$D_{\dot{x}}$	500 kg m^{-1}
$D_{\dot{y}}$	800 kg m^{-1}
r	0.2 m
Maximum forward velocity	0.5 m/s

Additionally, a thruster model according to [5] and [3] is utilised:

$$F = 0.4\rho d^4|n|n - \frac{1}{3}v_T\rho d^3|n| \tag{8}$$

where

- ρ is the density of water
- d is the diameter of the propellor
- n is the revolution speed of the thruster
- v_T is the velocity of the water going into the propellor

This information is used to generate the true motion of the vehicle given thrust through the water column, but for the subsequent ADCP localisation, this information has not been fused into the filter. The vehicle model is utilised to determine the predicted motion of the vehicle in the MPC algorithm to determine the control actions which minimizes the difference between the desired and predicted trajectory.

IV. Vertical descent simulation

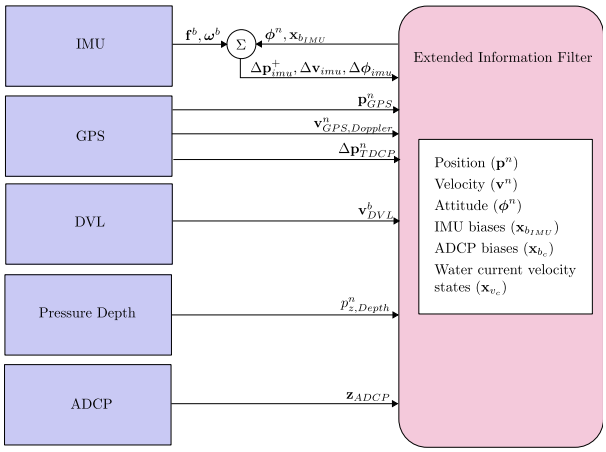

Fig. 2. The localisation architecture for the simulation with TDCP.

The Sirius AUV was simulated to descend with full thruster vertically (at 0.2m/s descent rate), and allowed to be perturbed by a simulated spacially varying water current profile, with nominal horizontal currents of about 4 cm/s. The pose of the vehicle, along with the water current profile observable with the ADCP sensor, is being estimated according to the method outlined in [9]. The desired trajectory is a completely vertical trajectory from the sea surface. The descent occurs over 200 seconds, and 40m of depth. Table I lists parameter values used for the simulation.

TABLE I
PARAMETER VALUES USED IN THE SIMULATION

GPS receiver	Lassen iQ GPS receiver
Initial GPS position fix accuracy	10 m ($2\sigma_p$)
Initial GPS velocity accuracy	0.04 m/s ($2\sigma_v$)
AUV descent rate	0.2 m/s
ADCP make and model	RDI 1200 kHz
ADCP measurement uncertainty	0.02 m/s ($2\sigma_a$)
ADCP range	30 m
Water current depth cell size	1 m
Simulation time	200 seconds
Simulated depth	70 m
ADCP update rate	3 Hz

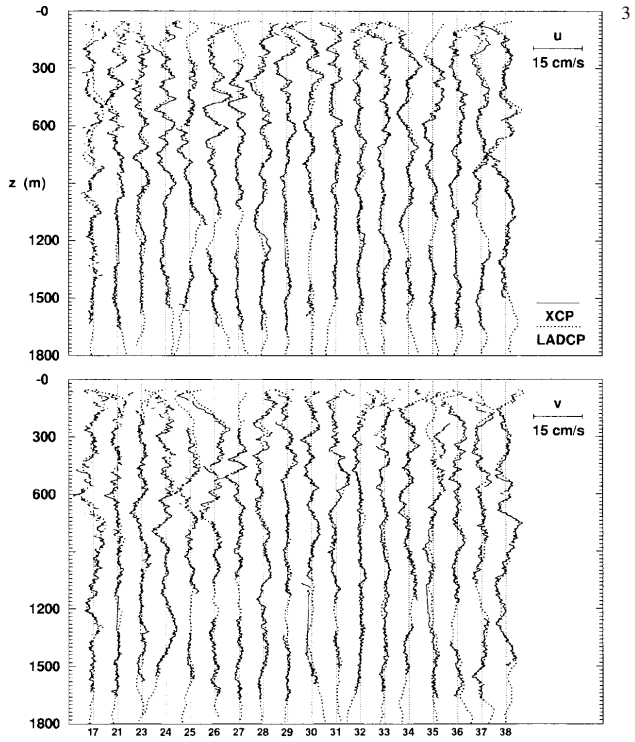

Fig. 3. Results for Lowered acoustic Doppler current profiler (LADCP) velocity profiles (dotted lines) and higher-resolution expendable current profiler (XCP) measurements (solid lines) in u (north) and v (east) directions. The y-axis represents depth, and the x-axis represents separate current profiling missions [12].

A tactical-grade Honeywell HG1700A58 IMU (1 degree/hr bias stability) was simulated, providing position, velocity and attitude constraints through the integration of the body rotation rates and accelerations. The method used to incorporate the inertial measurements into the filter are similar to [6], with further additions in [8]. For the GPS, Time Differenced Carrier Phase (TDCP) [13] is also assumed to be available in addition to GPS position and Doppler velocity. TDCP is a particular implementation of carrier phase processing of the GPS signal. It can be approximately modelled as tracking the change in position of the vehicle. The TDCP measurement is assumed to have an uncertainty of 10 mm/s (2σ). Figure 2 outlines the localisation architecture for this simulation.

A. Simulated Vertical Water Currents

The current profile is generated as a first order Markov process, to simulate correlated and randomly walking currents with depth, but with a bound on the random walk. The targeted behaviour of the water currents with depth is illustrated in Figure 3 [12]. The simulated current profile is shown in Figure 4, in which subsequent simulations will operate in.

B. MPC implementation

The MPC algorithm requires the computation of the Jacobian of the error function J in Equation 1 with respect to the optimised control actions τ_c, or $\frac{\partial J}{\partial \tau_c}$. The reference states in Equation 1 are defined as a vertical line directly below

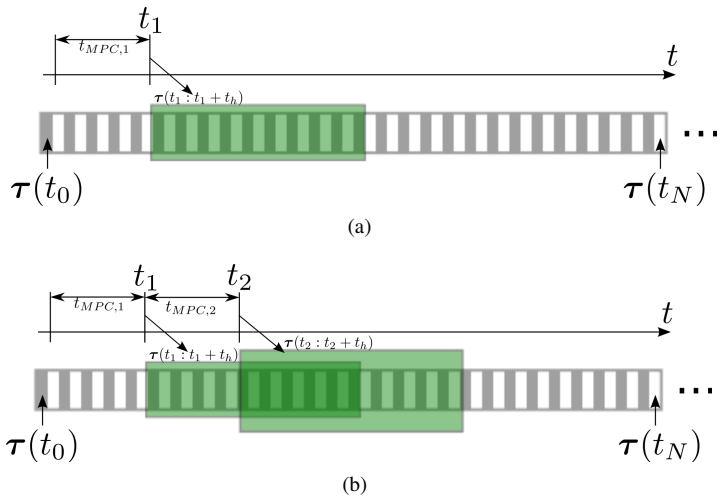

Fig. 5. The MPC algorithm as implemented has a certain computation time (t_{MPC}), which is accounted for in the simulation. In (a), at t_1 the optimisation stage calculated over $t_{MPC,1}$ has computed a set of control actions $\boldsymbol{\tau}(t_1 : t_1 + t_h)$, where t_h is the control horizon time. The thrusters are then actuated according to this set of control actions. For the next iteration, in (b), of the MPC algorithm over $t_{MPC,2}$, new control actions from t_2 which account for the receding control horizon from that point are calculated ($\boldsymbol{\tau}(t_2 : t_2 + t_h)$). The result is continually updated control actions as they are computed.

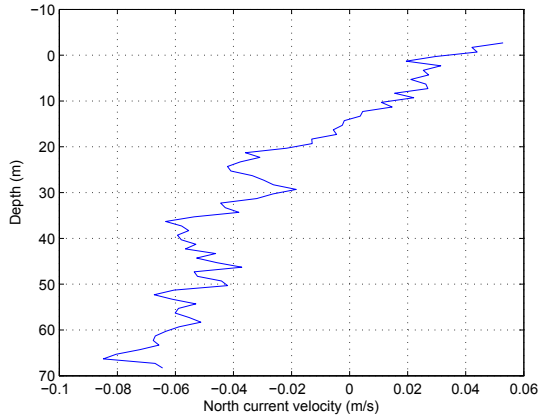

(a)

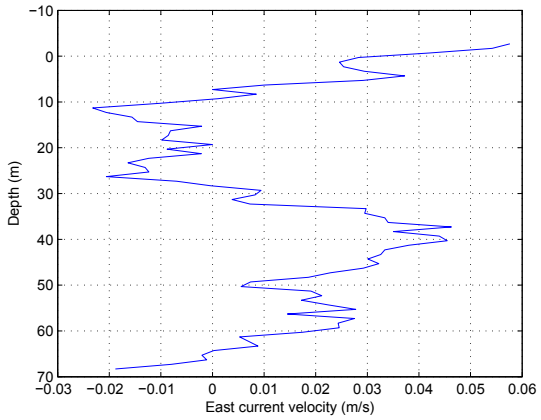

(b)

Fig. 4. The simulated current profile for the (a) north and (b) east velocity.

where the AUV initially descends. The control actions to be optimised are lateral thrust, as the vertical thruster is set to maximum during the descent. These Jacobians are derived numerically with Algorithm 1. The state ordering for the Jacobian is $[\mathbf{p}_{vm,k}, \mathbf{v}_{vm,k}, \psi_k, \omega_{vm,k}, \tau_c]$

The lsqnonlin function as implemented in the MATLAB Optimization toolbox [1] is applied to solve this optimization problem. Constraints such as a maximum thrust magnitude and maximum rate change of thrust must also be satisfied, and can be accommodated in the optimization step. Given the finite computation time of the MPC optimisation stage, there exists a delay between the information used in the MPC optimisation, and the actual implementation of control actions from this optimisation. This delay and how it is accommodated is outlined in Figure 5.

Control occurs in 0.3 second segments, to reduce computation and since the vehicle dynamics are slow. The lateral thrusters described by F_1 and F_2 in Equation 4 during the control horizon are to be optimised. A 2.5 and 5 second control horizon are compared to having no control (F_1 and F_2 are zero). Table IV-B outlines the computation time for the utilised control horizon times (on a Core 2 Duo 2.54 GHz).

Control horizon time (s)	Average optimization stage computation time (s)
2.5	0.40
5	0.71

C. Results

This section explores the results of the aforementioned simulation and MPC implementation. Figure 6 shows the trajectory following performance on the mean estimates from the localisation filter for various control horizons. Shown are the estimated north (Figure 6(a)) and east (Figure 6(b)) trajectory of the AUV in the simulation given no control, MPC with 2.5 seconds of control horizon, and 5 seconds of control horizon. The 5 second horizon time, even with

Algorithm 1 Jacobian creation for MPC

$N_c =$ Number of control actions to optimise
$J = \mathbf{0}_{(N_c+6)\times(N_c+6)}$
for $t < t_{MPC\,horizon}$ **do**

$$\begin{bmatrix} \ddot{x}_{b,k} \\ \ddot{y}_{b,k} \\ \ddot{\psi}_k \end{bmatrix} = \begin{bmatrix} (F_{1,k} + F_{2,k} - D_{\dot{x}}\dot{x}_{b,k}\,|\dot{x}_{b,k}| + M_y\dot{y}_b\omega_{vm,k})/M_x \\ (-D_{\dot{y}}\dot{y}_{b,k}\,|\dot{y}_{b,k}| + M_x\dot{x}_{b,k}\omega_{vm,t})/M_y \\ (F_{1,k}r - F_{2,k}r - D_{\dot{\psi}}\omega_{vm,k}\,|\omega_{vm,k}| - M_y\dot{x}_{b,k}\dot{y}_{b,k} + M_x\dot{x}_{b,k}\dot{y}_{b,k})/I_z \end{bmatrix}$$

$$\mathbf{v}_{vm,k+1} = \mathbf{v}_{vm,k} + \mathbf{R}_{b,k}^{b,0} \begin{bmatrix} \ddot{x}_{b,k} \\ \ddot{y}_{b,k} \end{bmatrix} \Delta t$$

$$\mathbf{p}_{vm,k+1} = \mathbf{p}_{vm,k} + \mathbf{v}_{vm,k+1}\Delta t$$

$$\omega_{vm,k+1} = \omega_{vm,k} + \ddot{\psi}_k \Delta t$$

$$\psi_{k+1} = \psi_k + \omega_{vm,k+1}\Delta t$$

$$\begin{bmatrix} \dot{x}_{b,k+1} \\ \dot{y}_{b,k+1} \end{bmatrix} = \mathbf{R}_{b,k}^{b,k+1}\left(\begin{bmatrix} \dot{x}_{b,k} \\ \dot{y}_{b,k} \end{bmatrix} + \begin{bmatrix} \ddot{x}_{b,k} \\ \ddot{y}_{b,k} \end{bmatrix} \Delta t\right)$$

$$F_{VM} = \begin{bmatrix} \mathbf{I}_2 & \mathbf{I}_2\Delta t & \mathbf{0}_{2\times(N_c+2)} & & \\ \mathbf{0}_{2\times2} & \frac{\partial \mathbf{v}_{vm,k+1}}{\partial \mathbf{v}_{vm,k}} & \frac{\partial \mathbf{v}_{vm,k+1}}{\partial \phi_{vm,k}} & \frac{\partial \mathbf{v}_{vm,k+1}}{\partial \omega_{vm,k}} & \frac{\partial \mathbf{v}_{vm,k+1}}{\partial \tau_{\mathbf{c}}} \\ & \mathbf{0}_{1\times4} & 1 & \Delta t & \mathbf{0}_{1\times N_c} \\ \mathbf{0}_{1\times2} & \frac{\partial \omega_{vm,k+1}}{\partial \mathbf{v}_{vm,k}} & 0 & \frac{\partial \omega_{vm,k+1}}{\partial \omega_{vm,k}} & \frac{\partial \omega_{vm,k+1}}{\partial \tau_{\mathbf{c}}} \\ & & \mathbf{0}_{N_c\times6} & & \mathbf{I}_{N_c} \end{bmatrix}$$

$J = F_{VM}\,J$
end for

a longer computation and hence t_{MPC}, results in less tracking error from the desired trajectory according to the localisation estimates due to the larger horizon time. The 2.5 second horizon time performs less accurately as the planning horizon is smaller, resulting in less optimal tracking for the full trajectory.

The total tracking error, as given to the MPC optimisation to minimize, is further compared in Figure 7 between the different scenarios. The tracking error is reduced given a higher horizon time, even with longer computation time. This implies that a longer computation time for the optimisation stage has negligible impact on the tracking performance compared to having a larger control horizon, since the dynamics of the control problem are slow. Given a more dynamic water current environment, a smaller planning horizon may give better performance, but in this static case, given the horizon time is longer than the computation time, better control tracking performance is possible.

Figure 8 shows the control actions from MPC with 2.5 seconds of control horizon. The controller is often saturating (at $\pm$62.5N), implying that the controller is being limited by the maximum thrust constraint. The large adjustments are required as the control horizon is small, and less control planning in the water current environment limits how optimally the control can occur. This is compared with the control actions from MPC with 5 seconds of control horizon showin in Figure 9. The controller is no longer saturating at $\pm$62.5N as often as the 2.5 second control horizon case. This shows that the controller action is not being limited by maximum thrust constraints. The smaller adjustments in control show that the control horizon time is adequate to account for the changing water currents that the vehicle will potentially encounter, without resorting to rapid corrections as in the 2.5 second control horizon case.

The true trajectory following performance including localisation error is shown in the north (Figure 10(a)) and east (Figure 10(b)) directions. The error is the addition of the tracking and localisation error, as the controller can only act on the mean estimates provided by the ADCP-aided localisation filter. The controller accuracy will approach the localisation error, at which point the localisation is the limitation on the trajectory following accuracy. Shown are the water current estimate errors and uncertainty estimates from the localisation filter in the north (Figure 11(a)) and east (Figure 11(b)) directions. This illustrates the uncertainty, and hence potential error in the water current estimates which are fed into the control algorithm. This error in vehicle and water current velocity, and hence position, during the descent is primarily dictated by the initial velocity error, with magnitude determined by the uncertainty, on the sea surface, as shown in [8]. The addition of USBL and LBL can further reduce the uncertainty in pose estimation to allow further improvements in trajectory following.

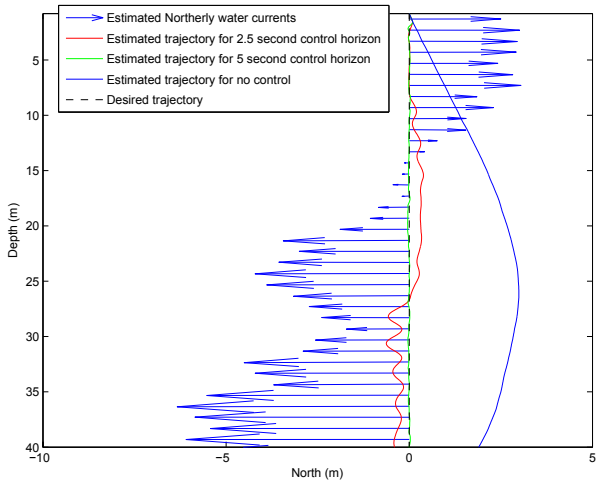

(a)

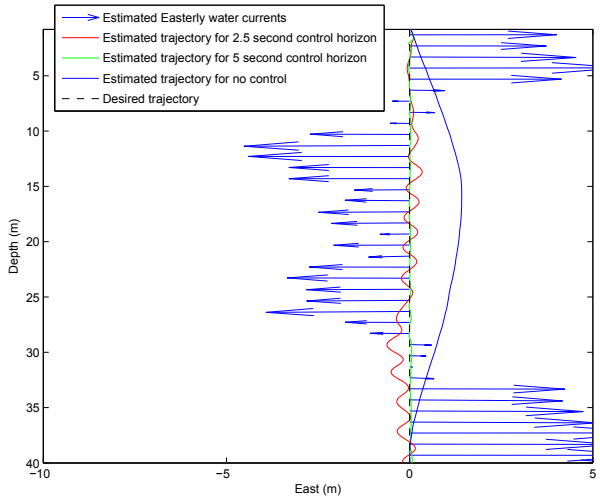

(b)

Fig. 6. The estimated (a) north and (b) east trajectory of the AUV in the simulation given no control, MPC with 2.5 seconds of control horizon, and 5 seconds of control horizon. The 5 second horizon time, even with a longer computation and hence t_{MPC}, results in less tracking error from the desired trajectory according to the localisation estimates due to the larger horizon time. The 2.5 second horizon time performs less accurately as the planning horizon is smaller, resulting in less optimal tracking for the full trajectory.

V. Conclusion

This paper has shown potential real time MPC control of an AUV in an *in situ* estimated water current profile. This enables control actions to allow trajectory following to account for the estimated water currents from the ADCP-aided localisation filter. Further work could look at applying MPC to more difficult to control AUVs and real-time implementation on a real AUV. The optimal time for the control horizon depends on ocean current conditions and the system response of the vehicle, and determining this is an area of future work. Additionally, more sophisticated realisations of the MPC algorithm, including variable reference points and analytical Jacobians, can further improve the performance of the control algorithm, with potential methods outlined in [4].

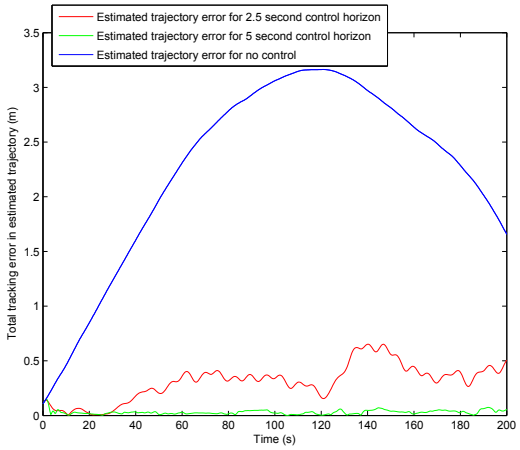

Fig. 7. The total tracking error for the trajectory given no control, MPC with 2.5 seconds of control horizon, and 5 seconds of control horizon. The tracking error is reduced given a higher horizon time, even with longer computation time.

References

[1] T.F. Coleman, M.A. Branch, and A. Grace. *Optimization toolbox*. MathWorks, 1999.

[2] R. Findeisen and F. Allgöwer. An introduction to nonlinear model predictive control. In *21st Benelux Meeting on Systems and Control*, volume 11, 2002.

[3] T.I. Fossen. Guidance and control of ocean vehicles. *New York*, 1994.

[4] P.W. Gibbens and E.D.B. Medagoda. Efficient model predictive control algorithm for aircraft. *Journal of guidance, control, and dynamics*, 34(6):1909–1915, 2011.

[5] A.J. Healey, SM Rock, S. Cody, D. Miles, and JP Brown. Toward an improved understanding of thruster dynamics for underwater vehicles. *Oceanic Engineering, IEEE Journal of*, 20(4):354–361, 1995.

[6] Todd Lupton and Salah Sukkarieh. Efficient integration of inertial observations into visual slam without initialization. In *Intelligent Robots and Systems, 2009. IROS 2009. IEEE/RSJ International Conference on*, pages 1547–1552, Oct. 2009.

[7] S.C. Martin and L.L. Whitcomb. Preliminary results in experimental identification of 3-dof coupled dynamical plant for underwater vehicles. In *OCEANS 2008*, pages 1–9. IEEE, 2008.

[8] L. Medagoda, Jakuba M.V., Pizarro O., and Williams S.B. Water Column Current Profile Aided Localisation for Autonomous Underwater Vehicles. In *OCEANS 2010*, Sydney, Australia, 2010. IEEE.

[9] L. Medagoda, S.B. Williams, O. Pizarro, and M.V. Jakuba. Water Column Current Aided Localisation for Significant Horizontal Trajectories with Autonomous Underwater Vehicles. In *IEEE OCEANS 2011, Kona*, September 2011.

[10] P.Z. Molenaar. Model predictive control to autonomous helicopter flight, 2007.

[11] W. Naeem, R. Sutton, and SM Ahmad. Pure pursuit guidance and model predictive control of an autonomous underwater vehicle for cable/pipeline tracking. In *Proceedings-Institute of Marine Engineering Science and Technology Part C Journal of Marine Science and Environment*, pages 25–35. The Institutde of Marine Engineering, Science and Technology, 2004.

[12] K. Polzin, E. Kunze, J. Hummon, and E. Firing. The finescale response of lowered adcp velocity profiles. *Journal of Atmospheric and Oceanic Technology*, 19(2):205–224, 2002.

[13] B.K.H. Soon, S. Scheding, H.K. Lee, H.K. Lee, and H. Durrant-Whyte. An approach to aid INS using time-differenced GPS carrier phase (TDCP) measurements. *Gps Solutions*, 12(4):261–271, 2008.

[14] S.B. Williams, O. Pizarro, I. Mahon, and M. Johnson-Roberson. Simultaneous Localisation and Mapping and Dense Stereoscopic Seafloor Reconstruction Using an AUV. In *Experimental Robotics*, pages 407–416. Springer, 2009.

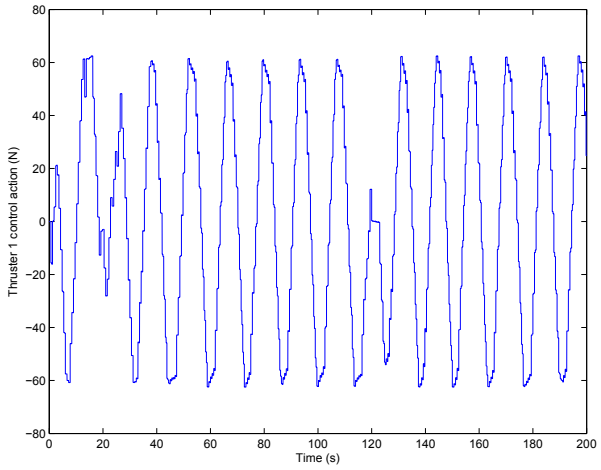

(a)

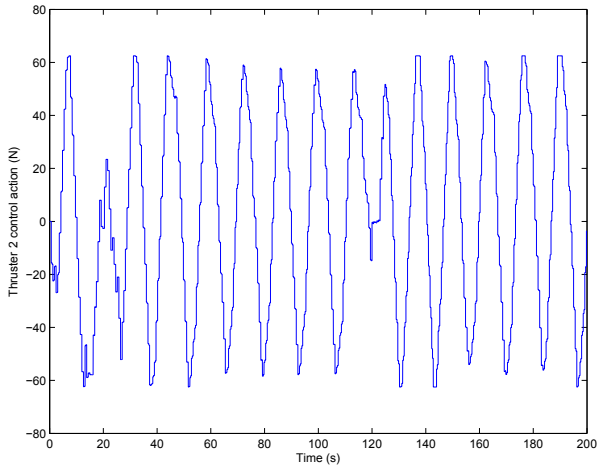

(b)

Fig. 8. The control actions from MPC with 2.5 seconds of control horizon. The controller is often saturating (at ± 62.5N), implying that the controller is being limited by the maximum thrust constraint.

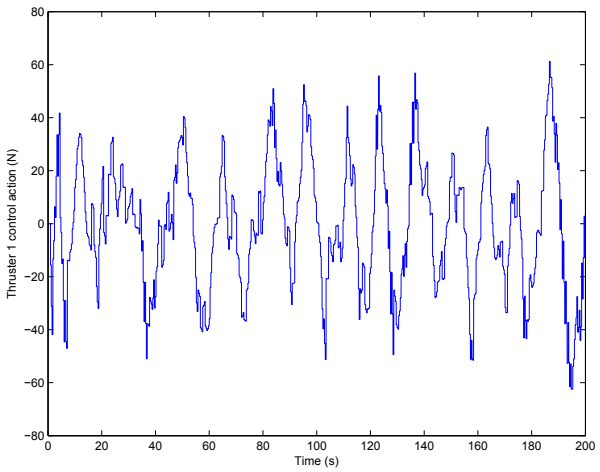

(a)

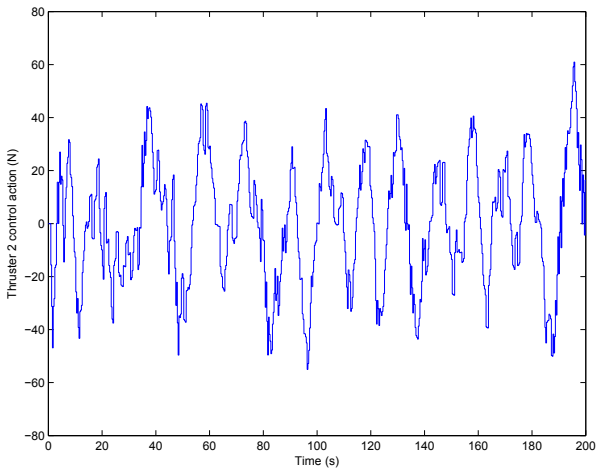

(b)

Fig. 9. The control actions from MPC with 5 seconds of control horizon. The controller is no longer saturating at ± 62.5N as often as the 2.5 second control horizon case.

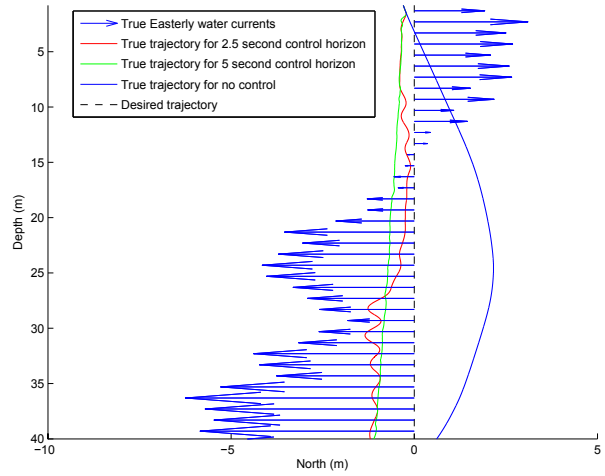

(a)

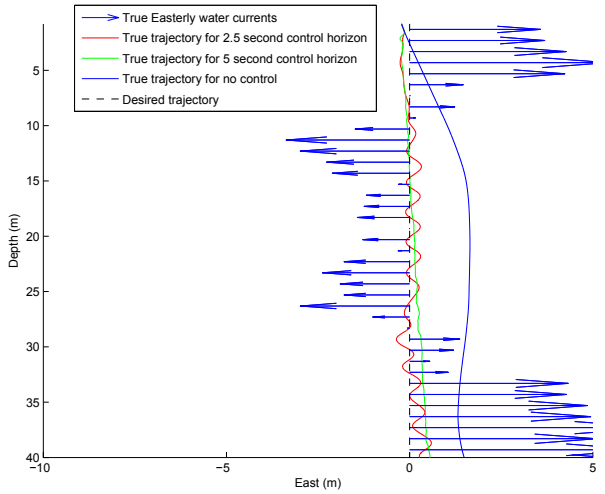

(b)

Fig. 10. The true trajectory following performance including localisation error is shown in the (a) north and (b) east directions. The error is the addition of the tracking and localisation error, as the controller can only act on the mean estimates provided by the ADCP-aided localisation filter.

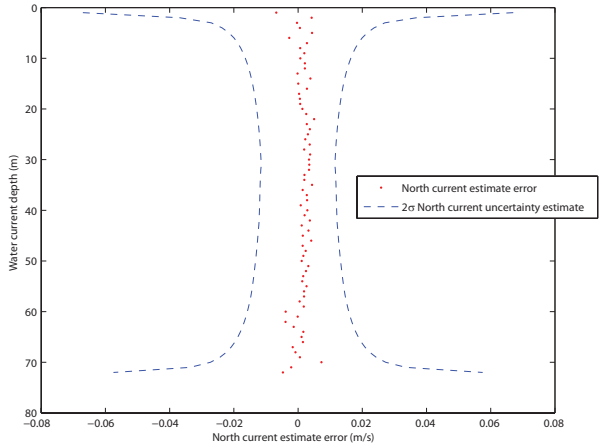

(a)

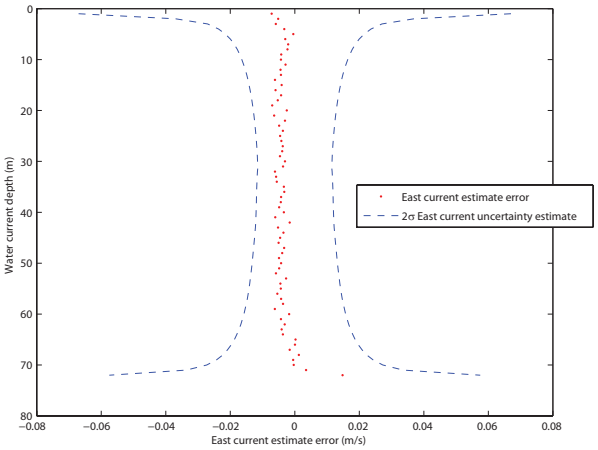

(b)

Fig. 11. Shown are the water current estimate errors and uncertainty estimates from the localisation filter in the (a) north and (b) east directions.